Effects of Pulse Current Charging in A Tri-electrode Rechargeable Zinc-air Flow Battery

Kanya Bumroongsil, Soorathep Kheawhom *

*Department of Chemical Engineering, Faculty of Engineering, Chulalongkorn University,Thailand, *E-mail:* Soorathep.K@chula.ac.th

Abstract

The challenging issues of an electrical rechargeable zinc-air battery that must be resolved include: dendritic growth of zinc and hydrogen evolution reaction (HER). To mitigate these issues, pulse current charging with flowing electrolyte shows high potential. Herein, a mathematical model of a tri-electrode rechargeable zinc-air flow battery is developed and validated against experimental data. The model is then applied to find the optimal conditions for enhancing the performance of the battery. Results showed that increasing zinc ion concentration on the surface of zinc significantly decreases HER. Moreover, when charging with constant high current density, zinc ion concentration on the zinc surface suddenly decreased; thus resulting in an increase in HER. In comparison, pulse current charging at the same current density can retard the diffusion-controlled by reducing the concentration gradient of zinc ion. In addition, the high flow rate of the electrolyte can maintain zinc ion concentration and suppress HER. It is also noted that sufficient zinc ion brings about high current efficiency and low degradation of the electrode. Results also indicated that greater efficiency of high current density charging can be attained by pulse charging applying low duty. Hence, pulse current charging with flowing electrolyte can improve both the performance and cyclability of the battery.

Keywords: pulse current, zinc-air battery, flow battery, hydrogen evolution reaction

1. Introduction

Zinc-air batteries show great potential to replace conventional secondary batteries. They exhibit high energy density, non-toxicity, good reversibility and are cost effective. Nevertheless, practical energy density produced by the battery is much less than the theoretical energy density. The critical issue lies in their unacceptable short

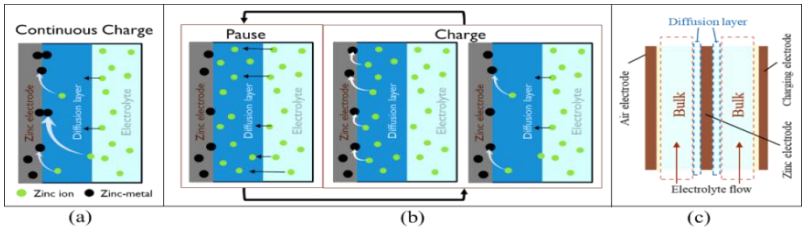

Fig.1 (a) and (b) show the difference between continuous charge and pulse charge: (a) occurrence of diffusion-controlled in continuous charge (b) prevention of diffusion-controlled by pulse charge process (c) the schematic of tri-electrode zinc-air battery.

life cycle. Hydrogen evolution reaction (HER) and dendritic growth on the zinc electrode are the main issues. Dendritic growth during recharge results from diffusion control on the zinc-electrode surface boundary (Fig.1a). Therefore, zinc ion concentration must be controlled to decrease the gradient at the electrode, thus preventing the diffusion-controlled process (Fig.1b).

Previous works have demonstrated using the pulse current charging to address dendritic growth problem and to extend the life cycle of the battery (Pichler, Berner et al. 2018). Riede, Turek et al. (2018) also conducted similar research and set up a model of a stagnant system battery during charging in a steady-state model. This work described the relationship between dendritic growth and the critical zinc ion concentration on the surface of the zinc electrode. However, the underlying mechanism of the conditions under a flowing electrolyte has not been discussed.

In this study, a zero-dimension model of a rechargeable tri-electrode zinc-air flow battery was developed and implemented in MATLAB. Consequently, the model developed was validated against experimental data. The model was then used to investigate the effects of pulse current charging and to compare the data with traditional constant current charging. Both zinc ion concentration and performances of the battery were examined. The operating factors investigated consisted of: electrolyte flow rate, mean current density and duty (on/off time) of pulsation.

2. Experimental

2.1 Material in experiment

The experiment was conducted by a tri-electrode zinc-air flow battery. The air electrode, zinc electrode, and charging electrode were fabricated in the battery case, which has an electrolyte flowing channel (Fig. 1c). The electrolyte was a solution of zinc oxide in 8M KOH. Both the zinc electrode and the charging electrode were made from nickel foam with an active area of 28 cm^2. A separator was placed between both electrodes. The separator was made by coating PVAc on a filter paper. The air electrode consisted of three layers with an active area of 28 cm^2. First, the outer layer, a gas diffusion layer, was made of 40% PTFE, 40% carbon and glucose. The middle layer contained Ni foam functioning as a current collector. The innermost layer was a catalyst layer made of 70% carbon and 30% manganese oxide. The air electrode was attached to a separator. This component was packed together in an acrylic case. The channel in the battery was filled with the electrolyte. The electrolyte flowed from below to upper, and then to the closed electrolyte tank (0.5 L) circulating into the bottom of the battery again etc.

2.2 Modelling method

The zero-dimension model was simulated by MATLAB software. The model was developed under assumptions including: no heat generation or consumption and the occurrence of zinc-metal at the surface of the electrode; the zinc-metal does not flow out of the battery. The model was assumed to neglect convective transfer between the electrodes and volume change of the electrolyte. Cell voltage and current density were evaluated in the tri-electrode zinc-air flow battery model. The I-V curve consisted of consecutive charge steps starting from 0 mA/cm^2 with holding time of 60 s. At the end

of holding time, cell potential was taken to plot the polarization curves. The model validation was carried out using the experiment data.

2.3 Studied parameters

The effects of zinc ion concentration at the surface electrode on the performance of the battery were investigated by dynamic simulation. Parameters studied included electrolyte flow rate, mean current density and duty of pulse charging. The aim was to find the optimum operating parameters.

3. Model and description

Table 1 Reaction in the zinc-air battery during discharge

Reaction	Equation	E^0 (V)
Oxygen reduction reaction (reaction A)	$1/2O_2 + H_2O + 2e^- \leftrightarrow 2OH^-$	0.4
Dissolution (reaction B)	$Zn + 4OH^- \leftrightarrow Zn(OH)_4{}^{2-} + 2e^-$	-1.2
Precipitation	$Zn(OH)_4{}^{-2} \leftrightarrow ZnO + 2OH^- + H_2O$	-
Overall reaction	$2Zn + O_2 \leftrightarrow 2ZnO$	-
HER (reaction C)	$2H_2O + 2e^- \rightarrow H_2 + 2OH^-$	-0.83
Parasitic reaction	$Zn + 2OH^- + 2H_2O \rightarrow Zn(OH)_4{}^{-2} + H_2$	-

In Table 1, the reactions of the discharging process are described. The basic principle of the battery involves the oxidation of zinc and the reduction of oxygen from air. During charging, reactions take place in the opposite direction. HER consumes electrolyte and zinc leading to self-corrosion and reduces zinc utilization.

3.1 Material balance

Fig.1c concerns the material balance equation for each electrolyte boundary:
where i is bulk and air, s is surface of zinc electrode. The dissolved species k in the electrolyte are OH^-, $Zn(OH)_4{}^{-2}$and H_2O.
The material balance equation is given accordingly as in Eq. (1):

$$\frac{dC_k}{dt} = \frac{1}{V_e{}^i}\left[F_{k,in} - F_{k,out} + J_k + j_k^{dif,s} + \sum_r \nu_k^r R_k^r\right] \quad (1)$$

where, C_k^i is the concentration of species k in the i boundary, $V_e{}^i$ is the electrolyte volume in i boundary. $F_{k,in}$ and $F_{k,out}$ are the molar flow rate of species k in and out the bulk electrolyte. For the air boundary and electrode surface, these are zero. ν_k^r and R_k^r are the stoichiometric coefficient and the reaction rate of production or consumption of species k in reaction r. The molar transfer of dissolved species is expressed below, as in Eqs. (2) and (3). J_k is rate of molar transfer across the electrode of species which consists of diffusion and migration. $j_k^{dif,s}$ is rate of diffusion transfer of species k from the bulk electrolyte to diffusion layer on the zinc electrode surface.

$$J_k = \left(D_k \frac{C_k^{air} - C_k^{bulk}}{\delta_{sep}} \cdot \varepsilon_{sep} \cdot A_{sep}\right) + \left(\frac{t_k}{z_k F} \cdot i^{cell} \cdot \varepsilon_{sep} \cdot A_{sep}\right), \; j_k^{dif,s} = D_k \frac{C_{k,s} - C_{k,b}}{\delta_{k,dif}} \cdot A_{zn} \quad (2), (3)$$

where D_k is the diffusion coefficient of species k. δ_{sep}, ε_{sep} and A_{sep} are the properties of separator which are thickness, porosity and area, respectively. t_k is transference number of ion k. i^{cell} is applied current density. The thickness of diffusion layer is calculated by Sherwood number (Sh), as shown in Eqs. (4) and (5):

$$\delta_{k,dif} = \frac{d_{eq}}{Sh}, \; Sh = 1.85\left(\frac{d_{eq}}{l} \cdot Re \cdot Sc\right)^{\frac{1}{3}} \quad (4), (5)$$

where, d_{eq} is hydraulic diameter, l is the length of the electrode, Re is Reynold number ($d_{eq}v\rho/\mu$), Sc is Schmidt number ($\mu/D_k\rho$), v, ρ and μ is velocity, density and viscosity of bulk electrolyte.

3.2 Cell potential (E_{cell})

Cell potential is calculated as in Eq. (6):

$$E_{cell} = E^{air} - E^{zn} - \eta_{ohm} \quad (6)$$

where E^{air} is the potential at the air electrode ($E_0^{air} - \eta_{act}^{air}$) and E^{zn} is the potential at the zinc electrode ($E_0^{zn} - \eta_{act}^{zn}$). The potential depends on concentration at the electrode surface and calculated as follows, according to Eqs. (7), (8) and (9):

$$E_0^{air} = E_0^{air,ref} + \frac{RT}{nF} ln\left(\frac{\left(C_{O_2}/C^{ref}\right)^{0.5}}{\left(C_{OH^-}^{air}/C^{ref}\right)^2}\right) \quad (7)$$

$$E_0^{zn} = E_0^{zn,ref} + \frac{RT}{nF} ln\left(\frac{\left(C_{Zn(OH)_4^{2-},s}/C^{ref}\right)}{\left(C_{OH^-,s}/C^{ref}\right)^4}\right), \quad E^H = E_0^{H,ref} - \frac{RT}{nF} ln\left(\frac{C_{OH^-,s}}{C^{ref}}\right) \quad (8), (9)$$

where $E_0^{air,ref}$ is the standard potential of air electrode, $E_0^{zn,ref}$ is the standard potential of zinc electrode, and C^{ref} is the concentration at reference state. According to a side reaction that occurred at zinc electrode, E^H is the potential of HER. $E_0^{H,ref}$ is the standard potential of HER.

3.3 Rate of reactions

In Table 1, the electrochemical reaction rates arise from reactions A, B and C. These reactions occur at the electrode surface. i_{air}, i_{zn} and i_H are current density regarding reactions A, B and C, respectively, multiplies with the area in which reactions occurred. The electrochemical reaction rates are expressed, as in Eqs. (10), (11) and (12):

$$R_A = i_{air} \cdot A_{air}/nF, \; R_B = i_{zn} \cdot A_{zn}/nF, \; R_C = i_H \cdot A_{zn}/nF \quad (10), (11), (12)$$

The charge transfer (i_{air}, i_{zn} and i_H) is described using Butler-Volmer equations (13), (14) and (15):

$$i_{air} = i_0^{air}\left[exp\left(\frac{\alpha_{air}nF}{RT}\eta_{act}^{air}\right) - exp\left(\frac{-(1-\alpha_{air})nF}{RT}\eta_{act}^{air}\right)\right], \; i_H = i_0^H\left[-exp\left(\frac{-(\alpha_H)nF}{RT}\eta_H\right)\right] \quad (13), (14)$$

$$i_{zn} = i_0^{zn}\left[\left(\frac{C_{OH^-,s}}{C_{OH^-,b}}\right)^4 exp\left(\frac{\alpha_{zn}nF}{RT}\eta_{act}^{zn}\right) - \left(\frac{C_{Zn(OH)_4^{2-},s}}{C_{Zn(OH)_4^{2-},b}}\right) exp\left(\frac{-(1-\alpha_{zn})nF}{RT}\eta_{act}^{zn}\right)\right] \quad (15)$$

The overpotential of HER is calculated as presented in Eq. (16):

$$\eta_H = \eta_{act}^{zn} - (E^{zn} - E^H) \quad (16)$$

The exchange current density (i_0) is the rate at equilibrium state. α is the transfer coefficient of the reaction. η is overpotential or activation loss of the reaction which is calculated from the total current of each electrode, according to Eqs (17) and (18):

$$\frac{d\eta_{act}^{zn}}{dt} \cdot C_{dl}^{zn} = i_{cell} - (i_{zn} + i_H), \quad \frac{d\eta_{act}^{air}}{dt} \cdot C_{dl}^{air} = i_{cell} - i_{air} \quad (17), (18)$$

3.4 Ohmic loss (η_{ohm})

Ohmic loss occurs due to ion transport resistance and resistance at zinc electrode and air electrode. These resistances are represented by R_{ohm}, as in Eq. (19):

$$\eta_{ohm} = i_{cell} \cdot A_{cell} \cdot R_{ohm} \quad (19)$$

4. Result and discussion

4.1 Model validation

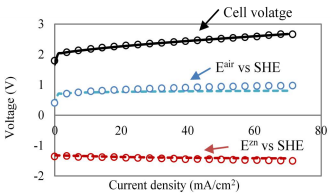

Fig.2 The charging polarization curve of the simulation (line) compared to the experimental data (dot) in condition: 8M KOH, ZnO 0.5M, flow rate 1.4 cm/s.

According to the battery model, some variables including i_0 and R_{ohm} must be chosen to fit the curve. The comparison of simulation data and experimental data is shown in Fig. 2. The cell voltage is calculated from Eq. (6). The electrode potentials are obtained from Eqs. (7) and (8) subtracted by their overpotentials. At high current density range, the electrode potential shows a small offset. This may be due to some proportion of ohmic loss that is not considered in this model. As for the cell voltage, the experimental data fitted in well and the result is most acceptable.

4.2 Effect of zinc ion concentration on the performance of battery

Insufficient zinc ion concentration can promote dendritic formation. Riede, Turek et al. (2018) found that dendrites appear as soon as a critical concentration (0.11M) is reached. To solve this problem, pulse method is applied. In Fig. 3a, the curve of concentration shows that pulse current can maintain zinc ion concentration at the surface while constant current rapidly consumes zinc ion. After 60s zinc ion concentration, under constant current charging, drops to 0.1M and then stabilizes. Thus, dendrite formation has the possibility to occur by constant current method. In Fig. 3b, the current density of HER which relates to the rate of corrosion can be suppressed using pulse current. It is also noted that the increase in HER results from the decreasing of zinc ion concentration at the surface. This result agreed well with the previous work of Lao-atiman, Bumroongsil et al. (2019). In addition, the higher electrolyte flow rate (black line) led to higher zinc ion concentration that maintained

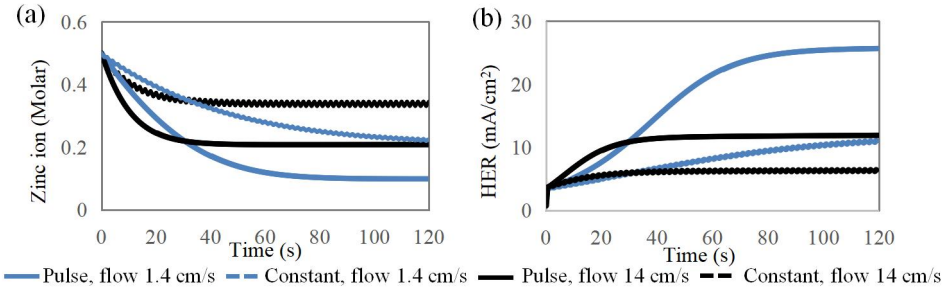

the zinc deposition reaction (backward reaction B) and suppressed the loss from HER.

Fig.3 The effect of pulse current as a function of electrolyte flow rate compared to constant current (a) on the zinc ion concentration at electrode surface (b) on the current density of HER in condition: 8M KOH, 0.5M ZnO, and current density 50 mA/cm^2.

4.3 Effect of current density and pulse duty on the current efficiency

The current efficiency, in this case, is defined by the equivalent current for zinc deposition divided by the total applied current $\left((2F \cdot N_{zn,deposited})/(i_{cell} \cdot A \cdot t)\right)$. The effect of corrosion, while pause charging, is not considered. As for the effect of current density in Fig. 4a, pulse charging spends more time to achieve the same capacity as constant current. At low current density, the efficiency of each method is not much different. Efficiency increases with current density. At high current density, the pulse method provides higher efficiency than the constant method. The highest efficiency (89.4%) is approached by duty of 0.25 pulse current method at 30 mA/cm^2. Pulse charging duty of 0.5 and 1 have the highest current efficiency: namely, 86.4% at 20 mA/cm^2 and

80.7% at 12 mA/cm^2, respectively. At high current density, pulse method can maintain more zinc ions on the surface by diffusion during off time. The constant charging method continuously consumes zinc ions. As mentioned previously, efficiency decreases due to lack of zinc ions at the electrode surface. In terms of mean current, pulse method applies charging current calculated by mean current/duty in order to reach the fixed capacity. In Fig. 4b, low mean current density (lower than 10 mA/cm^2) shows that the pulse method applied a higher current; thus resulting in higher efficiency, as seen in Fig 4a. As for the high mean current density, the efficiency of the pulse method decreased continuing close to the constant current but stabilized at a little higher level. Even though the lower duty had longer time to diffuse, the current while charging was also very high. However, low duty caused higher efficiency due to the zinc ions having longer time to diffuse from bulk to surface. The rate of zinc deposition was higher.

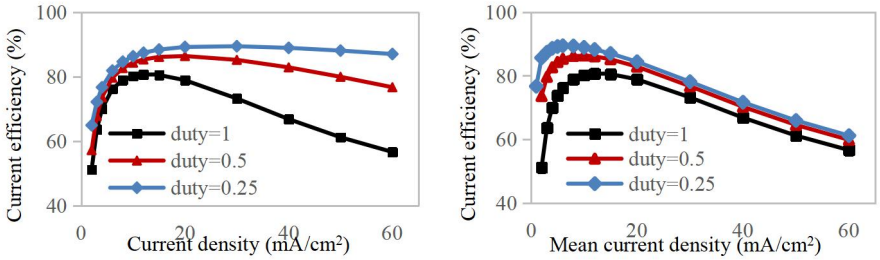

Fig.4 The effect of pulse current on the current efficiency at capacity 2 mAh/cm^2 as a function of duty (on time/(on time+off time)) (a) in case of current density (b) in case of mean current density in condition: 8M KOH, 0.5M ZnO and flow rate 1.4 cm/s.

5. Conclusion

In this work, the zero-dimension model of a tri-electrode rechargeable zinc-air flow battery was developed. Thus, constant current and pulse current charging processes were investigated. During recharge, zinc deposition was limited by diffusion-controlled, and zinc dendrite formed on the zinc electrode. However, it was found that by reducing zinc ion concentration gradient, pulse current charging with flowing electrolyte can suppress the issue. Moreover, sufficient zinc ion can decrease HER. In addition, it was found that the highest current efficiency was obtained by the pulse current method. In the case of high current density charging, pulse charging with longer time proved suitable. According to previous works, pulse current can suppress dendritic formation. As a result, both higher performance and longer life cycle of battery can be attained.

6. References

Lao-atiman, W., K. Bumroongsil, A. Arpornwichanop, P. Bumroongsakulsawat, S. Olaru and S. Kheawhom (2019). "Model-Based Analysis of an Integrated Zinc-Air Flow Battery/Zinc Electrolyzer System." **7**(15).

Pichler, B., B. S. Berner, N. Rauch, C. Zelger, H.-J. Pauling, B. Gollas and V. Hacker (2018). "The impact of operating conditions on component and electrode development for zinc-air flow batteries." Journal of Applied Electrochemistry **48**(9): 1043-1056.

Riede, J.-C., T. Turek and U. Kunz (2018). "Critical zinc ion concentration on the electrode surface determines dendritic zinc growth during charging a zinc air battery." Electrochimica Acta **269**: 217-224.